# A Study on Vortex Shedding From Spheres in a Uniform Flow

**H. Sakamoto**

**H. Haniu**

Department of Mechanical Engineering,
Kitami Institute of Technology,
Hokkaido, 090 Japan

*Vortex shedding from spheres at Reynolds numbers from $3\times10^2$ to $4\times10^4$ in a uniform flow was investigated experimentally. Standard hot-wire technique were used to measure the vortex shedding frequency from spheres in a low-speed wind tunnel. Flow-visualization experiments were carried out in a water channel. Important results from the investigation were that (i) the variation of the Strouhal number $St(=fD/U_0$, $U_0$: freestream velocity, D: diameter of the sphere, f: vortex shedding frequency) with the Reynolds number $(=U_0D/\nu$, $\nu$: kinematic viscosity) can be classified into four regions, (ii) the Reynolds number at which the hairpin-shaped vortices begin to change from laminar to turbulent vortices so that the wake structure behind the sphere is not shown clearly when a Reynolds number of about 800 is reached, and (vi) at Reynolds numbers ranging from $8\times10^2$ to $1.5\times10^4$, the higher and lower frequency modes of the Strouhal number coexist.*

## 1 Introduction

Wakes behind a sphere are encountered so frequently in engineering applications that large amounts of research have been conducted and massive amounts of data have been accumulated. Many reports which concern only the vortex shedding frequency from a sphere have been published. Möller (1938) has measured the frequency of vortex shedding from a sphere by flow-visualization in the Reynolds number range of $10^3<\mathrm{Re}<10^4$. He demonstrated that there are two Strouhal numbers in this Reynolds number range, i.e., a high-mode and a low-mode Strouhal number. Cometta (1957) measured the Strouhal number in the ranges of $10^3<\mathrm{Re}<4\times10^4$ using a hot-wire technique, and also found the same phenomenon. However, his conclusion that the two Strouhal numbers exist only when the sphere has a certain diameter is not very convincing from a hydrodynamic viewpoint. Achenback (1974) experimentally investigated on the Strouhal number by means of both the flow-visualization and hot-wire techniques, and demonstrated that the values for the higher frequency mode of Strouhal numbers showed the same results as those obtained by Möller at Reynolds numbers lower than $\mathrm{Re}=3\times10^3$. He also clarified that, when the Reynolds number is above $6\times10^3$, the vortices with the lower frequency mode are periodically shed from the sphere, and this phenomenon could be observed as far as the upper critical Reynolds number of $3.7\times10^5$. However, his measurement which used a hot-wire probe attached to the surface of the sphere failed to detect any low-mode Strouhal number in the range of the Reynolds numbers lower than $\mathrm{Re}=6\times10^3$. In other words, he did not succeed in confirming the existence of two Strouhal numbers in the ranges of $10^3<\mathrm{Re}<10^4$, as was reported by Möller and Cometta. Recently, Kim and Durbin (1988) performed experiments in the wakes of spheres for the Reynolds number range of $5\times10^2<\mathrm{Re}<6\times10^4$, and they found two distinct modes of unsteadiness which were associated with the small scale instability of the separating shear layer and with the large scale instability of the wake. In particular, they demonstrated that the higher frequency was detected only in the region of the wake immediately downstream of the sphere when the Reynolds number exceeded 800. Taneda (1978) examined the wake configuration formed behind a sphere in the range of $10^4<\mathrm{Re}<10^6$ by means of the flow-visualization methods. He clarified that the Strouhal number which was based on the wavelength caused by the alternate fluctuations of the wake was about 0.2 in the ranges of $10^4<\mathrm{Re}<3\times10^5$. Majumdar and Douglas (1970), Calvert (1972), Magarvey and Bishop (1961), and Pao and Kao (1977) also have measured the frequency of the vortex shedding from the sphere. However, they only measured in some limited ranges for the Reynolds number, and their results did not always coincide with one another.

Thus, many reports have been made concerning the vortex shedding from a sphere. The results, however, are fairly different from report to report. Therefore, it must be pointed out that reliable values for the Strouhal number in a wide range of the Reynolds numbers have not yet been found. This is due to the fact that the formation mechanism of the vortex for the change of the Reynolds number has not been properly clarified. Considering these facts described above, the present study is intended to measure the Strouhal number of a sphere by means of the hot-wire measurement for a wide range of the Reynolds numbers, including a low Reynolds number with a very low stream velocity. In particular, it closely examines the relationship between the wake configuration behind the sphere and the frequency of vortex shedding, observing its form through the flow visualization and concentrating on the high-mode and low-mode Strouhal numbers in the range of the Reynolds number of $10^3<\mathrm{Re}<10^4$.

Contributed by the Fluids Engineering Division for publication in the JOURNAL OF FLUIDS ENGINEERING. Manuscript received by the Fluids Engineering Division August 21, 1989.

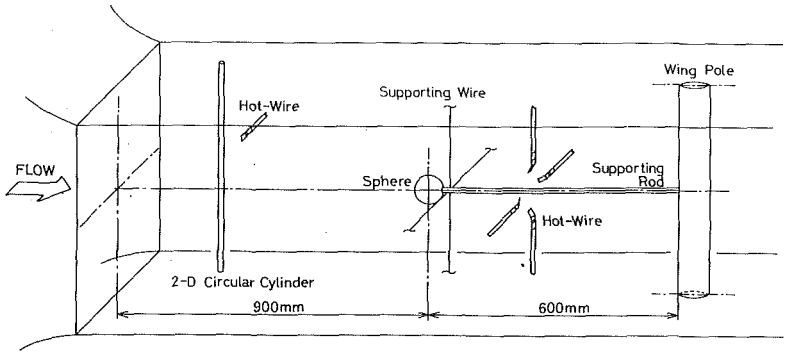


**Fig. 1 Sketch of sphere placed in test section**

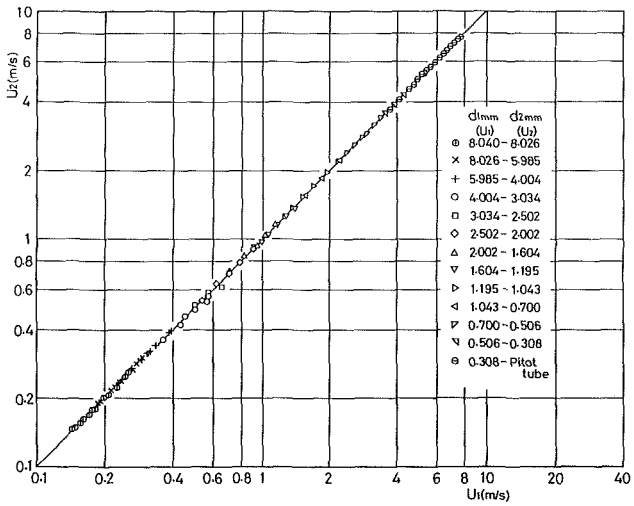


**Fig. 2 Calibration curve for velocity estimated from vortex shedding frequency of 2-D circular cylinder. (Uncertainty in $U_1$ and $U_2$: Less than ± 2 percent.)**

## 2 Experimental Apparatus and Procedure

**2.1 Experimental Apparatus.** The experiments were carried out in a suction-type wind tunnel with a 30cm by 30cm, 4m long working section and in a recirculating water channel whose test section had dimensions of 30cm in width, 40cm in depth, and 1.5m in length. Measurements for the frequency of the vortex shedding from the sphere were made by means of a hot-wire technique in the wind tunnel. The observation of the wake configuration for the sphere and a part of the measurements for the vortex shedding frequency were made in the water channel. The diameters, $D$, of the spheres selected for measurement were 20, 30, 40, and 60mm. The Reynolds number, $\mathrm{Re}(=U_0D/\nu)$, was varied not only by varying the freestream velocity, $U_0$, but also by using spheres of different diameters. Thus, the upper Reynolds number obtained in the present experiment was $5.5\times10^3$ in the water channel and $4\times10^4$ in the wind tunnel, respectively. In order to avoid interference by the support system, the sphere was supported at its rear by a small steel rod 3mm in diameter and 0.6m in length. The rod was fixed horizontally on the centerline of the test section by four fine cross-wires, 0.2mm in diameter, and a wing pole as shown in Fig. 1. The turbulence level in the freestream was below 0.2 percent at the wind tunnel and 0.1 percent at the water channel, and they did not vary noticeably with the change of the free-stream velocity.

**2.2 Measurement of Freestream Velocity.** In the wind tunnel test, it was difficult to measure the freestream velocity using a pitot tube or hot-wire anemometer when the velocity was lower than about 3 m/s. Therefore, when the free-stream velocity was lower than 3 m/s, it was estimated by using Roshko's formula (Roshko, 1956) based on the vortex shedding frequency of the regular mode from a two-dimensional circular cylinder mounted at the upstream of the test section. Since the vortex shedding of the regular mode from a two-dimensional circular cylinder is generated only in the limited range of the Reynolds numbers of $40<\mathrm{Re}<160$, thirteen cylinders whose diameters ranged from 0.3mm to 8mm were employed in accordance with the change in the freestream velocity. Also, in order to avoid the effect of the boundary layer along the tunnel wall on the frequency of vortex shedding from the circular cylinders, disks which were 7 to 10 times larger than the diameter of the cylinder were attached on both ends. Figure 2 shows a calibration curve for the velocity estimated from the vortex shedding frequency of the cylinder for each diameter. The calibration curve was produced using the following method: first, a relation between the reference velocity, $U_2$, measured by a pitot tube and $U_1$ obtained using the cylinder with a diameter of 0.308mm was found, secondly, a relation between the reference velocity, $U_2$, using the cylinder with the diameter of 0.308mm and $U_1$ using the cylinder with a diameter of 0.506mm was found, and then the relations between the reference velocity, $U_2$, and $U_1$ obtained using each cylinder were successively found in the same manner. Also, the circular cylinder which had been placed upstream of the sphere was removed from the test section during the measurement for the vortex shedding frequency of the sphere to avoid any influence on the flow characteristics. Furthermore, the freestream velocity in the test section of the water channel was obtained by measuring the time of travel for hydrogen bubbles passing a distance of 1m.

**2.3 Flow Visualization.** Flow around the spheres in the water channel were visualized using uranine dye. The injection of the uranine dye into the water channel was performed using a stainless tube with a diameter of 1mm. After the uranine dye was injected for specified period of time, the stainless tube was removed from the test section in order to avoid any disturbance generated by it.

## Nomenclature

$D$ = diameter of sphere
$F$ = nondimensional frequency of vortex shedding $=fD^2/\nu$
Re = Reynolds number $=U_0D/\nu$
St = Strouhal number $=fD/U_0$
$T$ = taking time for shedding of one hairpin-shaped vortex
$U_0$ = free stream velocity
$f$ = frequency of vortex shedding
$\nu$ = kinematic viscosity of fluid

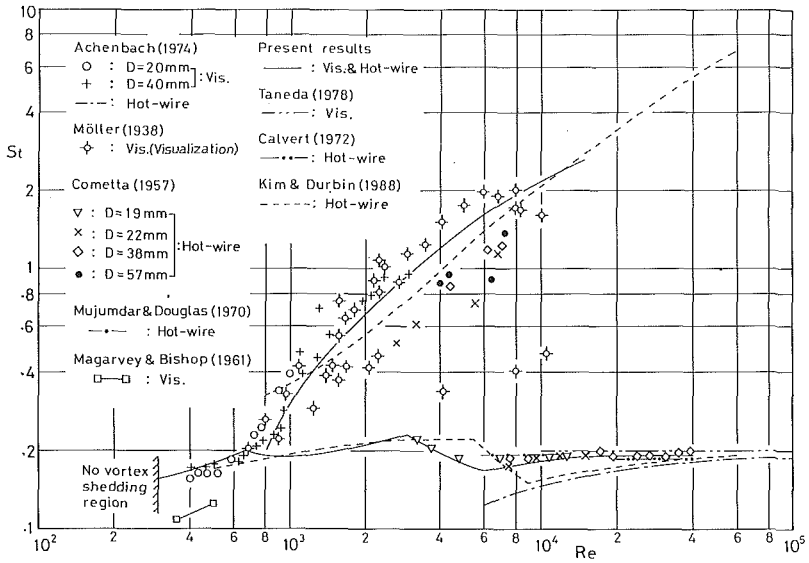


*Fig. 3 Various data for Strouhal number of sphere [1-8]*

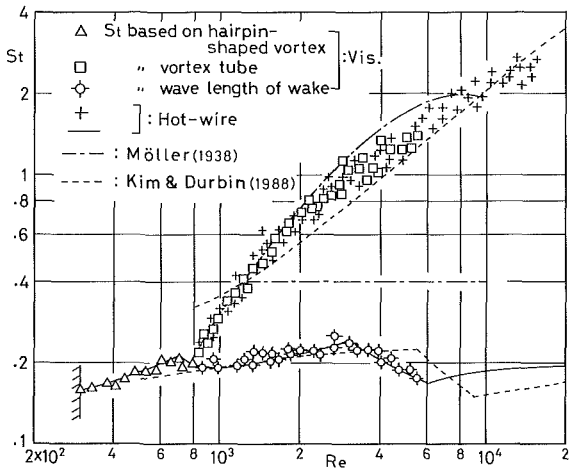


**Fig. 4 Distribution of low-mode and high-mode Strouhal number versus Reynolds number. (Uncertainty in St: less than ± 3.5 percent, in Re: less than ± 2 percent.)**

**2.4 Measurement of Frequency.** The frequency of vortex shedding from the sphere placed in the wind tunnel was determined on the basis of the power spectrum analysis of the fluctuating velocity detected by a hot-wire probe mounted in the wake behind the sphere. The position of the hot-wire probe (which was somewhat dependent on the Reynolds number) was determined by observing visualized patterns in the wake; it was in the range of (3 to 4)$D$ from the rear surface of the sphere. In order to avoid any influence from the hot-wire probe on the wake characteristics of the sphere, the prongs were made of pino-wire with a tip diameter of about 0.1mm and a length of 60mm; they were bent to a 135 degree angle and both ends of the hot wire were soldered of them. Also, the vortex shedding frequency of the sphere mounted in the water channel was determined by measuring the time necessary for a sequence of fifty vortices to be shed.

## 3 Results and Discussions

Figure 3 shows the main results that have been reported concerning the Strouhal number of a sphere $St(=fD/U_0$, where $f$ is the frequency of the vortex shedding, and $D$ the diameter of the sphere). The hairpin-shaped vortices begin to be periodically shed when the Reynolds number reaches about $Re=350\sim400$ (about $Re=300$ in the present experiment). The values of these Strouhal numbers up to $Re=10^3$ are almost the same as those previously recorded except for those obtained by Magarvey and Bishop (1961). In the range of the Reynolds numbers between $10^3$ and $10^4$, two Strouhal numbers exist, namely, the high-mode and low-mode Strouhal number. The high-mode Strouhal number obtained by Möller (1938) exists up to $Re=10^4$, but Cometta's result (Cometta, 1957) exists only up to $Re=7.4\times10^3$; these values are somewhat lower than those given by Möller. On the other hand, results obtained by Kim and Durbin (1988) show clearly that the two distinct modes exist simultaneously in the Reynolds number ranges of $8\times10^2<Re<6\times10^4$. In particular, it is noticeable that the high-mode St exists up to $Re=6\times10^4$. However, those values are somewhat lower than those obtained by Möller (1938) in the Reynolds number range of $10^3<Re<10^4$. Also, the value for the low-mode St obtained by Möller is a constant value of 0.4 in this range. When the Reynolds number is higher than about $10^4$, Mujumdar and Douglas (1970), Taneda (1978), and Calvert (1972) have reported that there exists only the low-mode St and it is a constant value of approximately $St=0.19\sim0.2$, although the results of Kim and Durbin (1988), and Achenback (1974) are a little different. Thus, in a range where Re is comparably small ($Re<10^3$) or large ($Re>10^4$), the Strouhal number obtained by the above researchers are mostly similar, while in the intermediate range of $10^3<Re<10^4$, the values differ considerably from researcher to researcher.

Figure 4 shows the values for the Strouhal number, St, obtained by the flow-visualization and hot-wire measurements in the present experiment at the range of the Reynolds numbers lower than $Re=1.5\times10^4$, in which there exist two Strouhal numbers, namely, the high-mode and low-mode St. When a Re of 300 is reached, the hairpin-shaped vortices begin to be periodically shed from the sphere, forming a laminar wake as shown in Fig. 8(*b*). When the Re is further increased to 800, the wake flow becomes turbulent with alternate fluctuations so that the configuration of the vortices is not clearly discernible as is shown in Fig. 8(*d*). In the Reynolds number range of $800<Re<10^4$, the Strouhal number determined on the basis of the wave length and velocity of the turbulent wake estimated from visual observation shows almost the same low-mode St as that which was obtained by the hot-wire measurements. This suggests that the low-mode St is caused by the progressive wave motion of the wake with alternate fluctuations. Moreover, when the Re is greater than 800, the pulsation is seen on

the vortex sheet separated from the sphere surface, and in accordance with its pulsation, the cylindrical vortices (defined as vortex tube in the present study) begin to be periodically shed, covering the vortex formation region as shown in Fig. 6(*a*). The values for the Strouhal number determined based on the frequency of the vortex tube shedding estimated from the visual observation are very similar to the high-mode St obtained by Möller (1938) and Achenbach (1974). This suggests

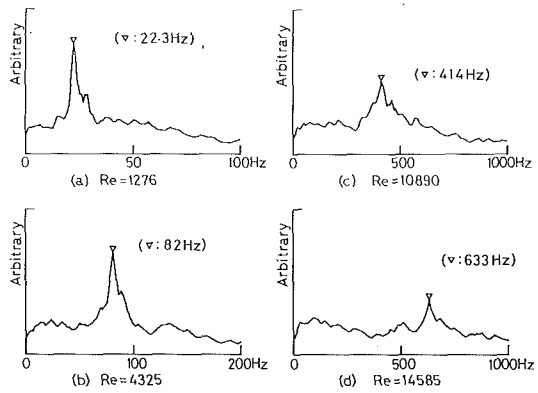


**Fig. 5 Power spectrum of fluctuating velocity based on vortex tube shedding (Uncertainty in Re: less than ±2 percent.)**

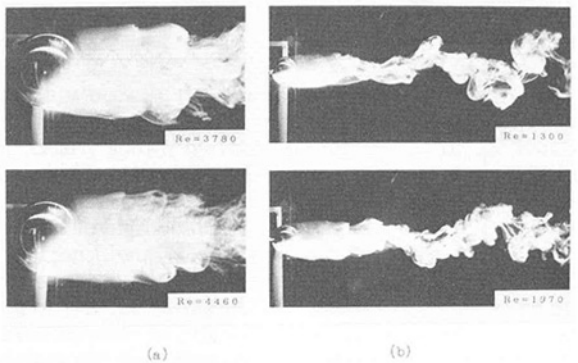


**Fig. 6 Visualized observation for wake behind sphere (*a*) Vortex tubes, (*b*) large-scale vortices. (Uncertainty in Re: less than ±2 percent.)**

that the high-mode St is based on the shedding of the vortex tube generated by the pulsations of the vortex sheet. Also, when a hot-wire is placed in the extreme neighborhood of the sphere, the frequency of the vortex tubes shed from the sphere could be detected by the spectrum analysis of the fluctuating velocity as shown in Fig. 5. On this spectrum analysis of the fluctuating velocity, the frequency of the large-scale vortex shedding which is considerably lower compared with that of the vortex tube is cut off by an analogue high-pass filter in order to appear only as a prevailing frequency based on the vortex tube. However, when the Re is larger than $1.5\times10^4$ in the present experiment, no clear peak is observed by the spectrum analysis because the fluctuation energy becomes extremely small. Furthermore, the energy level of the fluctuating velocity based on the shedding of the vortex tubes is much smaller than that based on wave motion of the wake with alternate fluctuations as shown in Fig. 6(*b*). Accordingly, it would be safe to consider that the unsteady flow around the sphere is mainly caused by the wave motion of the wake with alternate fluctuations when the Re is larger than about 800. On the other hand, Kim and Durbin (1988) have found that the high-mode St exists in the wide range of the Reynolds numbers between $8\times10^2$ and $6\times10^4$, and then it is associated with the small scale instability of the separating shear layer. However, they did not make clarifications concerning the structure of the small scale instability of the separating shear layer. Perhaps, it could be concluded that the vortex tube is formed by the small scale instability of the separating shear layer.

Figure 7 shows the Strouhal number based on the hairpin-shaped vortex and the large-scale vortex shedding obtained by the hot-wire measurement, namely the low-mode St, with the Reynolds number. We classified these results into regions I ~ VI and transitional regions A ~ C, taking into account the change in the Strouhal number corresponding to the Reynolds number. The following is a rough description of each region in terms of the relationship between its St and the configuration of the wake.

(i)Region I(300 < Re < 420)

According to Taneda's flow-visualization experiment in the range of 5 < Re < 300 (Taneda, 1956), when the Re is over 130, faint periodic pulsative motion with a very long period occurs at the rear of the vortex-ring formed behind the sphere, forming

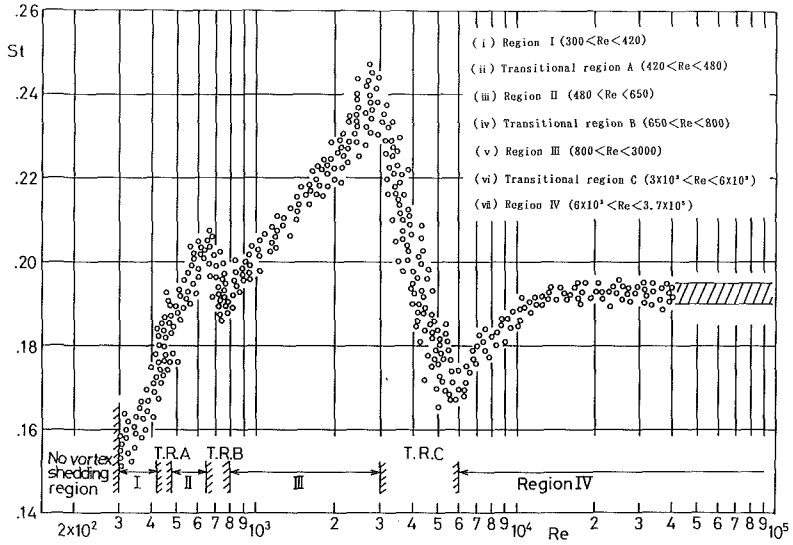


**Fig. 7 Strouhal number based on hairpin-shaped vortex and large-scale vortex shedding versus Reynolds number. For further information, see the caption of Fig. 4.**

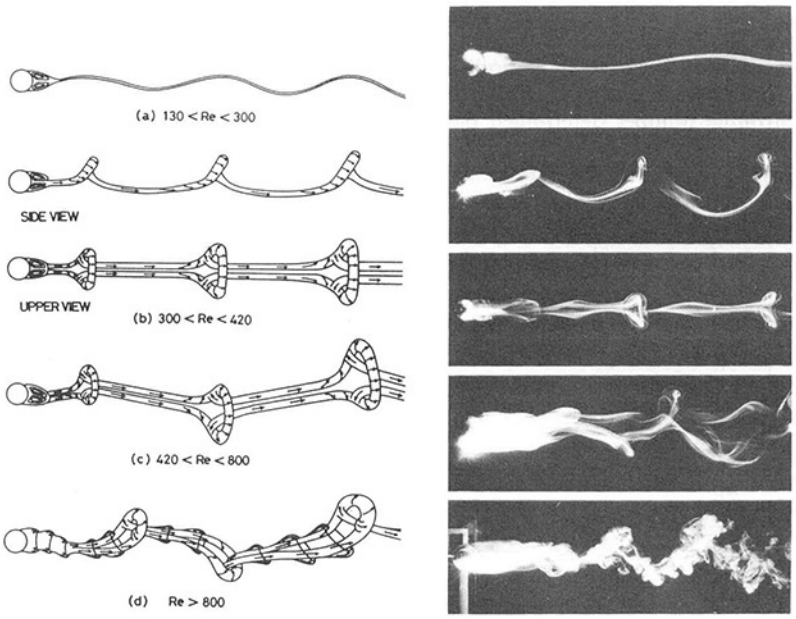


Fig. 8 Patterns of vortex shedding in wake at each region. For further information, see the caption of Fig. 6.

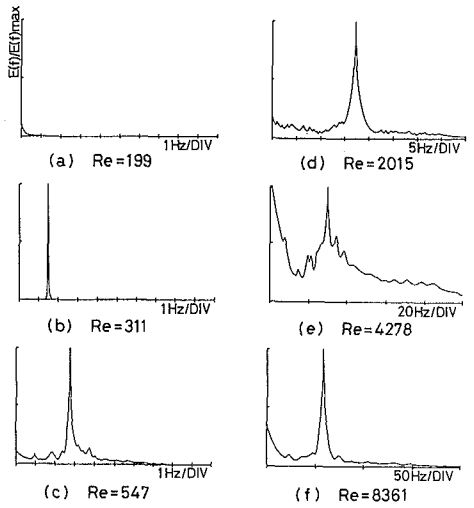


Fig. 9 Power spectrum of fluctuating velocity based on hairpin-shaped vortex and large-scale vortex shedding at each region. For further information, see the caption of Fig. 5.

a wavelike wake as shown in Fig. 8(*a*). Taneda also has reported that this phenomenon continues until a Reynolds number of about 300 is reached. Achenbach (1974), on the other hand, has reported that the wavelike wake turns into a so-called hairpin-shaped vortex when a Reynolds number of about 400 is reached. But, the present results which were measured by means of visual observation and spectrum analysis of the fluctuating velocity, as shown in Fig. 9 show that the hairpin-shaped vortex begins to be shed when the Re exceeds 300 (as shown in Fig. 9(*a*), there is no spectral peak in the power spectrum distribution when the Re is lower than 300). Taneda's report that a wavelike wake continues to be seen as far as the range of Re = 300 justifies the present results in which the hairpin-shaped vortices begin to be shed at Re = 300.

Figure 10 shows the waveform of the fluctuating velocity which was detected by the four hot-wire probes (CH 1 ~ 4) set at intervals of 90° on the circumference of a circular facet at a right angle in the wake behind the sphere. As the figure clearly shows, the amplitude of the waveform of the fluctuating

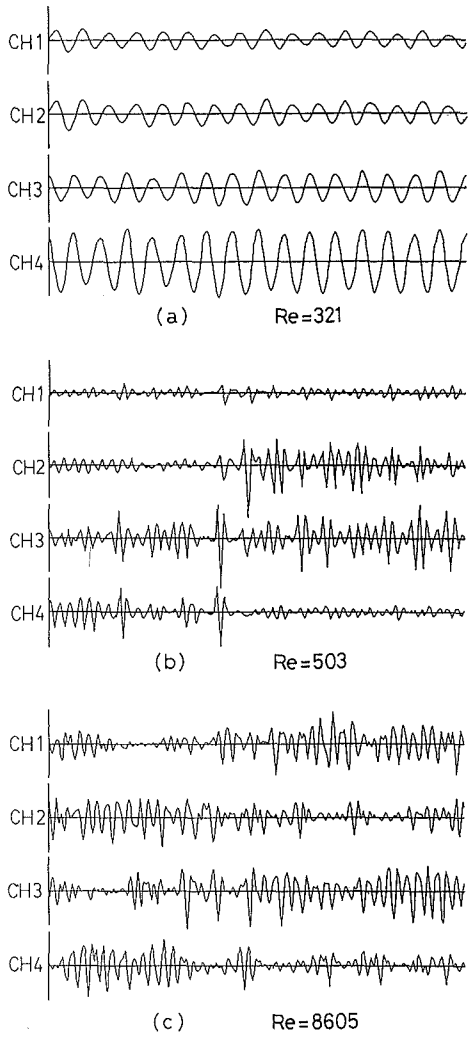


Fig. 10 Waveform of fluctuating velocity detected by four hot-wires equally spaced on circumference of a circle. (Uncertainty in bias error: less than ± 3 percent.)

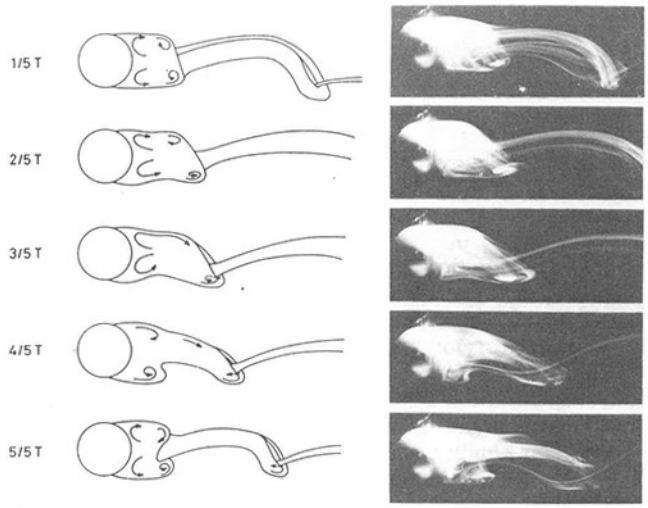


**Fig. 11 Shedding pattern of hairpin-shaped vortex with respect to one period**

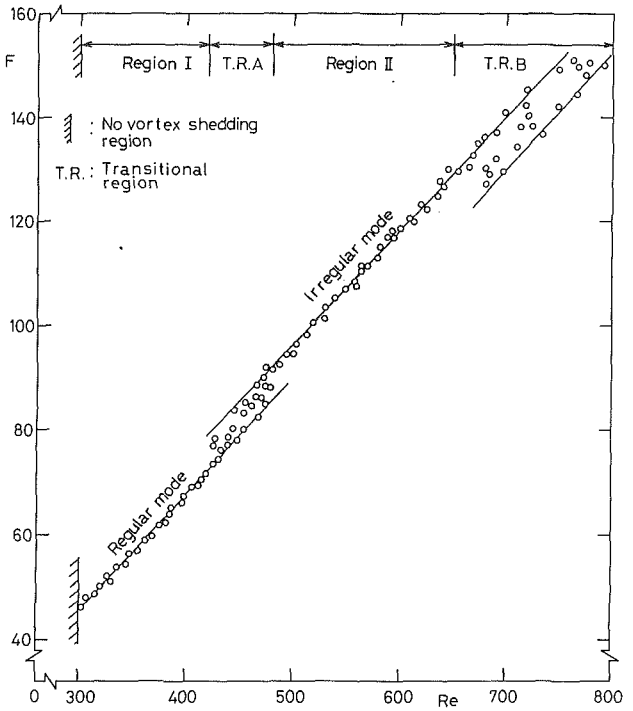


**Fig. 12 Non-dimensional frequency versus Reynolds number. (Uncertainty in *F*: less than ±3.5 percent, in Re: ±2 percent.)**

velocity detected by CH 4 is much larger than the others; this suggests that the hairpin-shaped vortices flow out in one direction from the point near where CH 4 is set. Moreover, the power spectrum as shown in Fig. 9(*b*) and the waveform of the fluctuating velocity as shown in Fig. 10(*a*) suggest that the hairpin-shaped vortices are periodically shed in what is called a regular mode with regularity in strength and frequency. This is perhaps because the energy entraining into the vortex formation region is very regularly supplied, stored and emitted, as is clearly shown by the shedding system of the vortex as shown in Fig. 11 (where $T$ is the time when one vortex is shed). This also explains why the vortices shed in succession are of the same strength and frequency.

(ii) Transitional Region A ($420 < \mathrm{Re} < 480$)

When the Re is greater than 420, the amplitude and waveform of the fluctuating velocity based on the shedding of the hairpin-shaped vortices begin to be generated with irregularity, and their shedding direction oscillates intermittently from left to right. The vortex shedding of the regular mode which existed in the previous region is also seen intermittently. Perhaps, regular and irregular modes appear alternately and last for a certain period of time in this region.

(iii) Region II ($480 < \mathrm{Re} < 650$)

When the Re exceeds 480, the waveform of the fluctuating velocity based on the shedding of the hairpin-shaped vortices becomes irregular as shown in Fig. 10 (*b*). In other words, the shedding pattern of the vortex is always in the irregular mode. This is perhaps because the supply, storage, and emission of energy within the vortex formation region becomes imbalanced so that the strength of the vortices shed from the formation region differs from one another. Furthermore, as is shown in Fig. 10(*b*), the amplitude of the fluctuating velocity differs from CH 1 ~ 4 as time passes; this suggests a change in the shedding point of the hairpin-shaped vortices. Accordingly, as Taneda (1978) has pointed out, the vortices are shed as if the facet including the vortices are rotating slowly and irregularly about an axis through the center of the sphere in the direction of the undisturbed flow.

Figure 12 shows the nondimensional frequency $F(=fD^2/\nu)$ in terms of the frequency, $f$, of the hairpin-shaped vortex shedding. According to Roshko (1974), Karman's vortex streets begin to be shed with regularity from a two-dimensional circular cylinder when a Re of about 40 is reached, and the shedding pattern becomes irregular when the Re approaches 160. Roshko has also reported that the non-dimensional frequency $F(=fd^2/\nu$, where $d$ is the diameter of the cylinder) is distributed on different straight lines in the regular and irregular modes with the Reynolds number. The nondimensional frequency, $F$, of the vortices shed from the sphere shows a similar property, i.e., it is regular in region I and irregular in region II, while the transitional region A is somewhere between the two regions. Furthermore, when the Re exceeds 650, the shedding pattern of the vortices is fairly different from that region II so that the non-dimensional frequency is distributed on a different straight line as shown in Fig. 12.

(iv) Transitional Region B ($650 < \mathrm{Re} < 800$)

As has already been previously described, when the Re exceeds 650, the cylindrical vortex sheet separated from the sphere surface shows pulsation, and the vortex tubes begin to be periodically shed in accordance with the pulsation as if covering the vortex formation region. These vortices diffuse near the sphere without retaining a cylindrical form. Also, the large-scale vortices flowing out from the formation region begin to change from laminar to turbulent vortices, thus obscuring their form.

(v) Region III ($800 < \mathrm{Re} < 3000$)

When the Re exceeds 800, some of the vortex tubes formed by the vortex sheet separating from the sphere surface flow into the vortex formation region at its rear end, while others are shed in small vortex loops. Some of the small vortex loops move downstream, intricately intertwining with the large-scale vortices which alternatingly flow out from the formation region as is shown in Fig. 6(*b*). As is clearly shown by the fluctuating waveform of Fig. 10(*c*), the point where the large-scale vortices are shed rotates slowly and irregularly since the amplitude detected by each hot-wire probe CH differs as the time elapses. And the large-scale vortices move away from the sphere rotating at random about an axis parallel to the flow through the center of the sphere; this has already been pointed out by Taneda (1978). The shape of the large-scale vortex has not yet been clarified. However, Perry et al. (1981) investigated the structure of turbulent wake behind an axis-symmetrical blunt body using a flying hot-wire apparatus, and clarified that it has the same structure as a hairpin-shaped vortex that is formed behind the blunt body in the low Reynolds numbers. Therefore, the large-scale vortex that flows out with alternate fluctuations away from the sphere may have the same structure as the

**Table 1** *Classification of vortex shedding pattern with respect to change of Reynolds number*

| Vortex shedding | No vortex shedding | Periodic vortex shedding | | | | | | | | | | | | | | No periodic vortex shedding |
|---|---|---|---|---|---|---|---|---|---|---|---|---|---|---|---|---|
| Orientation of the wake | | One way | Rolling | Irregular rotation of the plane containing the wake | | | | | | | | | | | | Rotation about streamwise axis |
| Configuration of the wake | Fixed vortex ring | Vortex loop | | Vortex tube | | | | | | | | | | | | Ω-shaped vortex |
| | | | | Waving wake | | | | | | | | | | | | |
| Region | No vortex shedding region | I | A | II | B | III | | | | C | | | IV | | | V |
| Reynolds number | $10^2$ 2 3 | 4 | 5 | 6 | 7 | 8 | 9 | $10^3$ | 2 | 3 | 4 | 5 | 6 | 7 | 8 | 9 $10^4$ 2 3 4 5 6 7 8 9 $10^5$ 2 3 4 5 6 7 8 9 $10^6$ |

hairpin-shaped vortex observed in the low Reynolds number region ($Re < 800$) whose model is shown in Fig. 8(*d*). Its structure has not yet been sufficiently clarified through detailed measurement concerning the structure of the turbulent wake behind the sphere. Therefore, it would be desirable to continue the investigation of the structure of the turbulent wake behind the sphere.

(vi) Transitional Region C ($3\times10^3 < Re < 6\times10^3$)

As is shown in Fig. 7, the Strouhal number decreases rapidly when the Re exceeds $3\times10^3$. In this region no evident peak is seen in the power spectrum distribution which has widely scattered values as shown in Fig. 9(*e*). This is perhaps because the vortex sheet which separates from the sphere surface changes from laminar to turbulent flow. The Strouhal number becomes smaller perhaps because it takes a longer time to store the necessary energy for the shedding of large-scale vortices since the dissipation of the energy increases in the turbulent vortex sheet so that the energy entraining into the vortex formation region decreases.

(vii) Region IV ($6\times10^3 < Re < 3.7\times10^5$)

When the Re exceeds $6\times10^3$, the vortex sheet separating from the surface of the sphere becomes completely turbulent. As is the case with the Karman vortex streets formed behind a two-dimensional body, the vortices shed from the formation region become stabilized when transition from laminar to turbulent flow occurs in the separated shear layer. Therefore, the alternate shedding of the large-scale vortices from the formation region also shows the pseudoregularity as is seen in the power spectrum distribution of Fig. 9(*f*). The Strouhal number based on the frequency of vortex shedding increases again with an increase in the Reynolds number until it becomes constant at $0.19 \sim 0.195$ when the Re exceeds $2\times10^4$. For the Strouhal number in the region where the Re is over the upper value of $4\times10^4$ studied in the present experiment, Achenbach has already reported that the Strouhal number which has a constant value of 0.19 exists as far as the region of $Re = 3.7\times10^5$; this is called the upper critical Reynolds number. Further, Taneda (1978) has clarified that when the Re exceeds the upper critical Reynolds number, the vortex sheets separating from the sphere flow out and roll up to form a pair of streamwise vortices without the periodic vortex shedding.

Table 1 shows the results of the present experiment for Reynolds numbers ranging from $10^2$ to $4\times10^4$, together with those obtained by Achenbach (1974), Kim and Durbin (1988), and Taneda (1978) at Reynolds numbers higher than $Re = 4\times10^4$. The table shows the change in the shape of vortices formed behind a sphere, the change in the direction of vortex shedding, and the existence or non-existence of the periodic vortex shedding in accordance with the change in the Reynolds number.

## 4 Conclusions

The present study has described an experimental investigation of the Strouhal number of the spheres by means of both the flow-visualization and hot-wire measurements in a wide range of the Reynolds number including the very low freestream velocity. The results led to be the following conclusions.

(1) The variation of the Strouhal number with the Reynolds number can be classified into four regions, and the relationship between the Strouhal number and the configuration of the wake in each region is clarified.

(2) When a Reynolds number exceeds about 300, the hairpin-shaped vortices begin to be periodically shed with regularity in its strength and frequency, forming laminar vortices until a Reynolds number is about 800.

(3) When a Reynolds number exceeds about 800, the hairpin-shaped vortices begin to change from the laminar to turbulent vortices with alternate fluctuations, this pattern of vortex shedding continues as far as the region of $Re = 3.7\times10^5$, which is called the upper critical Reynolds number.

(4) When a Reynolds number exceeds 800, the vortex tubes begin to be periodically shed covering the vortex formation region, in accordance with the pulsation of the vortex sheet separated from the surface of the sphere.

(5) At the Reynolds number ranging from $8\times10^2$ to $1.5\times10^4$ (which is some lower than that obtained by Kim and Durbin, 1988), the higher and lower frequency modes of the Strouhal number, which are caused by the periodic fluctuation in the vortex tube formed by the pulsation of the vortex sheet separated from the surface of the sphere and in the turbulent wake with progressive wave motion respectively, are coexisted.


## Acknowledgment

The authors express their sincere thanks to Mr. Y. Obata, Department of Mechanical Engineering, Kitami Institute of Technology, for his assistance in the construction of the experimental apparatus.


## References


Achenbach, E., 1974, "Vortex Shedding from Spheres," *J. Fluid Mech.*, Vol. 62, Part 2, pp. 209–221.

Calvert, J. R., 1972, "Some Experiments on the Flow Past a Sphere," *Aero. J. Roy. Aero. Soc.*, Vol. 76, pp. 248–250.

Cometta, C., 1957, "An Investigation of the Unsteady Flow Pattern in the Wake of Cylinders and Spheres Using a Hot Wire Probe," Div. Engng, Brown University, Tech.Rep. WT-21.

Kim, K. J., and Durbin, P. A., 1988, "Observation of the Frequencies in a Sphere Wake and Drag Increase by Acoustic Excitation," *Phys. Fluids*, Vol. 31, No. 11, pp. 3260–3265.

Magarvey, R. H., and Bishop, R. L., 1961, "Wakes in Liquid-Liquid Systems," *Phys. Fluids*, Vol. 4, No. 7, pp. 800–805.

Möller, W., 1938, "Experimentelle Untersuchung zur Hydromechanik der Kugel," *Phys. Zeitschrift*, Vol. 39, No. 2, pp. 57–80.

Mujumdar, A. S., and Douglas, W. J. M., 1970, "Eddy Shedding from a Sphere in Turbulent Free Streams," *Int. J. Heat Mass Transfer*, Vol. 13, pp. 1627–1629.

Pao, H. P., and Kao, T. W., 1977, "Vortex Structure in the Wake of a Sphere," Phys. Fluids, Vol. 20, No. 2, pp. 187–191.

Perry, A. E., and Watmuff, J. F., 1981, "The Phase-Averaged Large-Scale Structures in Three-Dimensional Turbulent Wakes," *J. Fluid Mech.*, Vol. 103, pp. 33–51.

Roshko, A., 1956, "On the Development of Turbulent Wakes from Vortex Streets," N.A.C.A Report, No. 1191.

Taneda, S., 1978, "Visual Observations of the Flow Past a Sphere at Reynolds Numbers Between $10^4$ and $10^6$, *J. Fluid Mech.*, Vol. 85, Part 1, pp. 187–192.

Taneda, S., 1956, "Studies on the Wake Vortices (III). Experimental Investigations of the Wake Behind a Sphere at Low Reynolds number," *Res. Inst. Appl. Mech.*, Kyushu University, Fukuoka, Japan, Report No. 4, pp. 99–105.